Viscoelastic Continuum Model of Nonpolar Solvation. 1. Implications for Multiple Time Scales in Liquid Dynamics

Mark Berg[†]

Department of Chemistry and Biochemistry, University of South Carolina, Columbia, South Carolina 29208

Received: July 8, 1997[⊗]

A continuum model of nonpolar solvation is presented. Coupling of the solute to the solvent is assumed to occur through a change in the solute's size or shape upon electronic excitation. Both spherical and nonspherical changes in the solute are treated. The time-dependent shear and longitudinal moduli of the solvent determine the solvation response function. Unlike prior continuum models of solvation, both a rapid, viscosity-independent inertial component and a slower, viscosity-dependent diffusive component emerge from the model, even when only one time scale is assumed in the moduli. The origin of multiple time scales in this model, which has a single solvent coordinate with complex dynamics, is contrasted with treatments such as the multimode Brownian oscillator models, which postulate multiple solvent coordinates, each with simple dynamics.

I. Introduction

Relaxation on multiple time scales has long been recognized as a key feature in the dynamics of high-viscosity liquids.[1] However, early work on dynamics in low-viscosity liquids often focused on a single relaxation time. Continuum models are found to be a surprisingly successful first approximation to these dynamics.[2] More recently, both improved experiments and computer simulation have shown that a second "inertial" time scale exists in addition to the previously recognized "diffusive" time scale.[3−7] This paper shows that the existence of these two time scales and their most prominent experimental features can be predicted from a continuum model, at least for nonpolar solvation. Although continuum models have obvious limitations in describing real systems with molecular structure, their simplicity is a major advantage in discussing the qualitative physics underlying the model. This paper contrasts the "dynamical" origin of multiple time scales embodied in the continuum model with other "spectroscopic" explanations.

The general features of liquid dynamics are mirrored in electronic state solvation. When a solute molecule undergoes a change in electronic structure, either due to progress along a reaction coordinate or due to a change in electronic state, the surrounding solvent undergoes a time-dependent reorganization to optimize the solvation of the new electronic structure. Solvation mechanisms are broadly classified as "polar" when solvent molecule reorientation is predominant, as occurs with dipole−dipole interactions with a polar solvent,[8−17] and "nonpolar" when solvent molecule center-of-mass motion is predominant.[18−26]

In the case of nonpolar solvation, transient hole-burning experiments have established the basic time scales involved.[26−34] At high viscosity, a rapid, subpicosecond relaxation is clearly separated from a slower relaxation. The rapid component is approximately viscosity independent. It remains subpicosecond in the high-viscosity supercooled liquid and even persists in the glassy solid. In the solid, this component results from interactions with the phonons of the environment. In the liquid, experiments have shown that the rapid component is the high-temperature extrapolation of the phonon-induced relaxation in the solid. Because of this specific experimental assignment, we refer to the rapid component of nonpolar solvation as the "phonon-induced" component, rather than using the less specific term, "inertial". Computer simulation has also shown that this component can include weak oscillations,[23] although current experiments have not been able to test this prediction.

In contrast to the phonon-induced component, the slower component's relaxation time is directly proportional to the solvent viscosity. In the glass, this component does not relax at all but is responsible for static inhomogeneous broadening of electronic transitions. We have assigned this component to reorganization of the structure that supported the phonon-like motion during the earlier phonon-induced relaxation. Because of this assignment, we have used the specific term "structural" relaxation, instead of the more general description "diffusive" relaxation.

In addition to these experimental results, there have been several theoretical studies of nonpolar solvation dynamics. Walsh and Loring looked at the first stage of solvation and its effect on photon echo experiments with a ballistic treatment.[18] Ladanyi and Stratt have looked at the early portion of solvation using an instantaneous normal mode analysis.[19] Larsen et al. have explored connections between nonpolar solvation and vibrational relaxation using the same method.[20] Kalbfleisch, Ziegler, and Keyes used a similar approach to look at solvation in high-pressure gasses.[21] Evans also looked at the first steps of solvation using kinetic theory.[22] Stephens, Saven and Skinner have used approximations based on dropping certain high-order correlation effects to look at nonpolar solvation on a complete range of time scales.[23,24] Bagchi has examined the correlation function of the total ground-state potential energy, which is closely related to the solvation correlation function, using density functional theory.[25]

This paper presents a continuum model for nonpolar solvation. A change in the solute's effective size or shape upon electronic excitation is assumed to be the primary interaction driving nonpolar solvation. Following excitation, the solvent must move to allow the solute cavity to expand. This movement is modeled

[†] Tel: (803) 777-1514. Fax: (803) 777-9521. Email: berg@psc.sc.edu.
[⊗] Abstract published in *Advance ACS Abstracts,* December 15, 1997.

S1089-5639(97)02206-8 CCC: $15.00
Published on Web 01/01/1998

by treating the solvent as a viscoelastic continuum. The solvation reponse function is then calculated from the time- or frequency-dependent mechanical moduli of the solvent. This model is an analog of continuum models of polar solvation, which predict solvation dynamics from the frequency-dependent dielectric constant.[8−17]

Although microscopic theories clearly deal with the effects of liquid structure more realistically than continuum models, there are several important advantages to a continuum model of solvation. Despite the neglect of liquid structure, continuum models are frequently found to capture a surprising amount of the essential physics involved and have been very influential in the development of more sophisticated theories of liquid dynamics.[35] Continuum models are generally regarded as providing an excellent approximation to processes such as molecular reorientation[2] and polar solvation[8,9] on times longer than a picosecond. Zwanzig and Bixton[36] followed by Metiu, Oxtaby, and Freed[37] showed that a viscoelastic continuum model of the velocity autocorrelation function works well, even on the 100 fs time scale. Because continuum models require relatively simple input data, they are often easier to compare to experimental data than microscopic theories. The continuum model of solvation presented here has already been compared to experimental data over a broad range of temperature in supercooled liquids.[26,32,33] The simplicity of continuum models also gives a readily apparent conceptual picture of the dynamics involved.

Despite the early success of continuum models, even at very short times,[36,37] there is currently much discussion in the literature characterizing inertial dynamics as fundamentally "single molecule" or at least intimately connected to molecular structure. This paper shows that although molecular structure is important for describing the details of inertial dynamics, the basic features are contained within a continuum picture.

In part, this discussion arises because earlier continuum models of solvation did not predict the existence of inertial dynamics. The model of nonpolar solvation presented here shows that this limitation is not fundamental to a continuum treatment but is due to the details of implementing the model. In the current model, a full equation of motion is written for the solvent displacement as a function of time and position. The time dependence of the displacement comes both from the time/frequency dependence of the moduli and from inertial terms in the equation of motion. Approximations could be used to relate the experimental observable directly to the solvent moduli. These approximations avoid the complexities of a full equation of motion, but only at the expense of losing the inertial effects.

The relative simplicity of this model is exploited to make three major points concerning the physical origin of inertial and diffusive relaxation. First, the existence of an inertial component in solvation dynamics is not essentially connected with molecular structure or single molecule motion. Structural effects are preeminent only in an even shorter "ballistic" time regime. Second, this model attributes the existence of two times scales to two stages of relaxation, first by coherent phonon emission and then by viscous flow to relieve shear stress, occurring along a single solvent coordinate, the cavity radius. This explanation contrasts with approaches such as multimode Brownian oscillator models,[38] which assign different time scales to distinct solvent coordinates. Third, the time-dependent results of the model are transformed to frequency-domain spectral densities to test the idea that a spectral representation gives an accurate picture of a set of underlying solvent modes. This model provides an example in which the observed spectral density is not closely related to such a set of modes.

The discussion of these points is predicated on the assumption that the viscoelastic model is a good first-order description of the important physical porcesses involved, an assumption that is supported by several other studies. This model has already been used to quantitatively fit temperature-dependent solvation data in two different systems.[26,32] Oscillations in the response function, which have been seen in computer simulation under some conditions,[23] are explained by this model. Computer simulations of electron solvation have also identified the solvent's response to changes in the size and shape of the solute as major components of the solvation process,[39−41] and this model gives quantitative fits to those simulations.[42]

Although certain formulas resulting from this model have been used in analyzing experimental data,[26,32,33] the details of its derivation have not been published previously. The effects of changes in shape, in addition to changes in size, are incorporated into the model presented here. These results have not appeared before.

The detailed description of the model and the development of the equations implementing it are contained in section II. The solution of these equations in outlined in the Appendix, and the general properties of the solutions are discussed in section III. Section IV discusses how phonon-induced and structural relaxations are obtained as long- and short-time limits of the full solution. Section V examines the validity of the approximate decomposition of the complete solution into the sum of a phonon-induced and a structural component. An exact decomposition of the solution is presented to highlight the important distinction between decomposing a response function into two components and having those two components behave independently as conditions change. A discussion of the differences between the current "dynamical" approach to explaining the multiple time scales in liquids and the "spectroscopic" approach used in other models is contained in section VI. A final summary is presented in section VII.

II. Definition of the Model

A. Overview. The solute is modeled as a nearly spherical cavity within a viscoelastic continuum representing the solvent (Figure 1). The boundary between solute and solvent is sharp and acted on by two sets of forces: one from the solvent tending to collapse the cavity and one from the solute resisting the collapse. Before $t = 0$, the solute is in the ground electronic state, and the cavity radius equilibrates at a certain size. At $t = 0$, the solute is transferred to the excited electronic state, instantaneously increasing (or decreasing) the solute forces on the cavity boundary. To regain equilibrium, the cavity must expand (contract). This expansion (contraction) lowers the system energy and causes a solvation-induced Stokes shift.

The solute forces include the direct forces from the solvent−solute intermolecular potential and the free energy of organizing the solvent molecules around the solute cavity (i.e., the "surface tension"). The change in the solute force at $t = 0$ is caused by the difference in the solvent−solute potential between the ground and excited states. Many different specific mechanisms may be responsible for this difference: changes in repulsive forces generated by the overlap of the molecular cores, changes in internal bond lengths, changes in dispersion (polarizability−polarizability) interactions, changes in dipole−polarizability interactions, and so on. All of these "nonpolar" mechanisms produce forces that are strongly concentrated in the first layer of solvent and that act primarily between the centers-of-mass

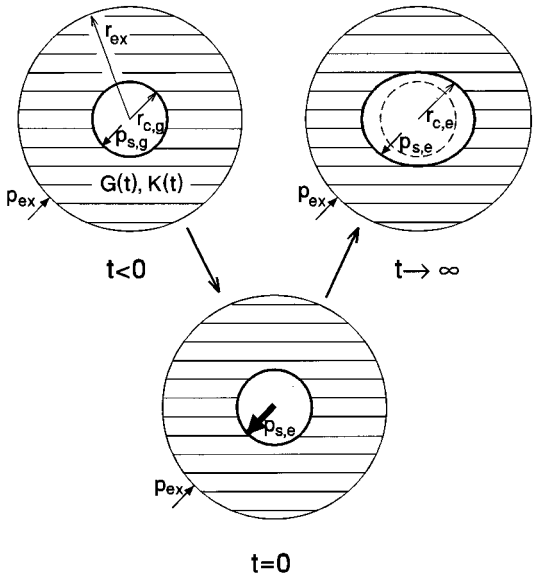

Figure 1. Schematic illustration of the boundary conditions of the model. The solute occupies the central cavity (heavy line). A viscoelastic solvent (lined region) fills the space between the solute and the external boundary. For $t < 0$, the balance of forces on the cavity boundary determines the cavity radius at equilibrium in the ground state. At $t = 0$, the solute jumps to its excited state, and the outward pressure from the solute changes. As $t \rightarrow \infty$, a new equilibrium cavity size and shape are established. See the text for the definition of the parameters.

of the solute and solvent. They are all treated equivalently within the model as a change in the radial force on a sharp cavity boundary. The model does not incorporate "polar" solvation mechanisms such as dipole-dipole[8,10] or dipole−quadrupole interactions.[43] These interactions are inherently long-range and produce primarily torques rather than center-of-mass forces.

The forces on the cavity boundary from the solvent include the equilibrium external pressure and the nonequilibrium forces generated in response to changes in the solute. The core of this model is calculating the nonequilibrium forces from the equation of motion for a viscoelastic continuum. From these forces, the time dependence of the cavity radius is calculated and then translated into the time dependence of the electronic transition energy.

B. Definition of Viscoelastic Quantities. The central quantities of interest in this model are the mechanical stress and strain tensors.[44,45] The stress tensor σ is defined as the force **F** per unit area **A**

$$\mathbf{F} = \sigma\mathbf{A} \tag{1}$$

The tensor notation incorporates both compressive forces acting perpendicular to the area and shear forces acting parallel to the area. In an isotropic material, only two tensor quantities are independent: the scalar isotropic pressure

$$p = -{}^1/_3 \operatorname{Tr} \sigma \tag{2}$$

and the second-rank shear stress tensor

$$\sigma^{(2)} = \sigma + pI \tag{3}$$

where I is the unit matrix.

The movement of the solvent in response to these forces is given by the displacement **u** relative to a reference state. The strain tensor is defined as the symmetric spatial derivative of the displacement

$$\epsilon_{ij} = \frac{1}{2}\left(\frac{\partial u_i}{\partial x_j} + \frac{\partial u_j}{\partial x_i}\right) \tag{4}$$

In isotropic material, the strain can also be decomposed into a scalar, compressive strain

$$\epsilon^{(0)} = \operatorname{Tr} \epsilon \tag{5}$$

and a second-rank shear strain

$$\epsilon^{(2)} = \epsilon - {}^1/_3\epsilon^{(0)} I \tag{6}$$

Standard mechanics posits a linear relationship between stress and strain, with moduli as the proportionality constants. In viscoelastic treatments, the magnitude of the moduli are allowed to vary with the duration of the stain.[44,45] Thus for the shear components of stress and strain

$$\sigma^{(2)}(t) = \int_{-\infty}^{t} 2\mu(t-t')\, \epsilon^{(2)}(t')\, \mathrm{d}t' \tag{7}$$

where $\mu(t)$ is the impulse shear response function and the factor of 2 is conventional. The time-dependent shear modulus is defined as the time-dependent force needed to maintain a step-function shear displacement

$$G(t) = \int_0^t \mu(t')\, \mathrm{d}t' \tag{8}$$

At short times, a liquid will resist a shear displacement with a modulus $G(t{=}0) = G_\infty$. With time, the resistance drops, and the modulus decays to zero, i.e., $G(t{=}\infty) = 0$. The viscosity observed at long times is

$$\eta = \int_0^\infty G(t)\, \mathrm{d}t \tag{9}$$

The compression impulse response function $\kappa(t)$ is similarly defined by

$$p(t) = \int_{-\infty}^{t} \kappa(t-t')\, \epsilon^{(0)}(t')\, \mathrm{d}t' \tag{10}$$

The time-dependent compression modulus

$$K(t) = \int_0^t \kappa(t')\, \mathrm{d}t' \tag{11}$$

has a nonzero value both at short times, $K(t{=}0) = K_\infty$, and at long times, $K(t{=}\infty) = K_0$.

Although the shear and compression moduli are the easiest to define, the model solutions are often most easily expressed in terms of the shear and longitudinal moduli. The longitudinal functions are defined by

$$\nu(t) = \kappa(t) + {}^4/_3\mu(t) \tag{12}$$

and

$$M(t) = K(t) + {}^4/_3 G(t) \tag{13}$$

With these definitions, the viscoelastic equation of motion is[44,45]

$$\rho\frac{\partial^2\mathbf{u}(t)}{\partial t^2} = \int_{-\infty}^{\infty}\{\nu(t-t')\nabla[\nabla\cdot\mathbf{u}(t')] - \mu(t-t')\nabla\times [\nabla\times\mathbf{u}(t')]\}\,\mathrm{d}t' \quad (14)$$

where ρ is the density. The term on the left represents inertial effects associated with the momentum of each volume element and is essential to describing wavelike motions in the solvent. This term contributes a time dependence to the solutions that is not included in the time dependence of the moduli themselves.

C. Boundary Conditions. The specific details of the model are contained in the boundary conditions (Figure 1). In its ground electronic state, the solute exerts a radial force per unit area $p_{s,g}(r_b)$ on the interior boundary. The magnitude of this force depends explicitly on the size of the cavity r_b. Setting this force equal to the solvent force at the boundary gives the condition

$$p_{s,g}(r_b) = -\int_{-\infty}^{t}\{2\mu(t-t')\,\epsilon_{rr}(r_b,t') + [\nu(t-t') - 2\mu(t-t')]\,\mathrm{Tr}\,\epsilon(r_b,t')\}\,\mathrm{d}t' \quad (15)$$

We also adopt slip boundary conditions; i.e., the solute exerts no tangential forces on the boundary

$$\epsilon_{r\phi}(r_b,t) = \epsilon_{r\theta}(r_b,t) = 0 \quad (16)$$

The outer boundary of the solvent at r_{ex} (Figure 1) experiences a constant external pressure p_{ex} that acts radially. The radius of the outer boundary is taken to infinity, giving the boundary conditions

$$p_{ex} = -\int_{-\infty}^{t}\{2\mu(t-t')\,\epsilon_{rr}(\infty,t') + [\nu(t-t') - 2\mu(t-t')]\,\mathrm{Tr}\,\epsilon(\infty,t')\}\,\mathrm{d}t' \quad (17)$$

and

$$\epsilon_{r\phi}(\infty,t) = \epsilon_{r\theta}(\infty,t) = 0 \quad (18)$$

Before $t = 0$, the system is in equilibrium with the ground state of the solute. This condition occurs when the solute pressure equals the external pressure

$$p_{s,g}(r_{c,g}) = p_{ex} \quad (19)$$

This equation defines the equilibrium cavity size in the ground state $r_{c,g}$. Under these conditions, the displacement of the solvent is

$$\mathbf{u}_{eq}(\mathbf{r}) = -\frac{p_{ex}}{3K_0}\mathbf{r}, \quad |\mathbf{r}| > r_{c,g} \quad (20)$$

measured relative to the system under zero pressure. The effect of the external pressure is removed by defining deviations from the equilibrium displacement and strain

$$\delta\mathbf{u}(\mathbf{r},t) = \mathbf{u}(\mathbf{r},t) + \frac{p_{ex}r}{3K_0}\hat{\mathbf{r}} \quad (21)$$

$$\delta\epsilon(\mathbf{r},t) = \epsilon(\mathbf{r},t) + \frac{p_{ex}}{3K_0}I \quad (22)$$

The initial conditions for these variables are simple: $\delta\mathbf{u}(\mathbf{r},0) = 0$ and $\delta\epsilon(\mathbf{r},0) = 0$.

For small displacements from the equilibrium cavity size, the solute force is assumed to vary linearly with the displacement of the cavity boundary

$$p_{s,g}(r_b) = p_{ex} - 3(K_s/r_{c,g})(r_b - r_{c,g}) \quad (23)$$

The force constant K_s is defined to have the units of a modulus and can be interpreted as the apparent compressibility of the solute cavity. In the excited state, the force constant is assumed to remain the same, but the equilibrium cavity size changes to $r_{c,e}$ (Figure 1)

$$p_{s,e}(r_b) = p_{ex} - 3(K_s/r_{c,g})(r_b - r_{c,e}) \quad (24)$$

We define a normalized solvent−solute coupling constant

$$C(\theta,\varphi) = \frac{r_{c,e} - r_{c,g}}{r_{c,g}} \quad (25)$$

To model changes in shape of the excited state, the coupling constant is allowed to be angle dependent. In the limit of weak coupling, $C(\theta,\varphi) \ll 1$, the deviations from a sphere will be small. As an approximation, the cavity will be treated as quasi-spherical in all other respects. With weak coupling, the cavity radii in the ground and excited states can be taken to be equal, $r_{c,e} \approx r_{c,g} \approx r_c$, whenever they do not occur as differences. To write eqs 23 and 24 in terms of the solvent displacement, note that $\delta u_r(r_b) = r_b - r_{c,g}$. The force laws in the ground and excited states become

$$p_{s,g}(r_c) = p_{ex} - 3(K_s/r_c)\delta u_r(r_c) \quad (26)$$

$$p_{s,e}(r_c) = p_{s,g}(r_c) + 3K_sC(\theta,\varphi) \quad (27)$$

These equations define a linear coupling between the solute electronic state and the solvent.

The change in solute force at $t = 0$ is incorporated as a time-dependent extension of the boundary condition in eq 15

$$p_{ex} - 3K_s[\delta u_r(r_c,t)/r_c] + 3K_sC(\theta,\varphi)\,H(t) = -\int_{-\infty}^{t}\{2\mu(t-t')[\epsilon_{rr}(r_c,t) - \mathrm{Tr}\,\epsilon(r_c,t)] + \nu(t-t')\,\mathrm{Tr}\,\epsilon(r_c,t)\}\,\mathrm{d}t' \quad (28)$$

$$H(t) = \begin{cases} 0, & t < 0 \\ 1, & t > 0 \end{cases} \quad (29)$$

Laplace transforms of time-dependent quantities

$$\bar{f}(s) = \int_0^{\infty} \mathrm{e}^{-st} f(t)\,\mathrm{d}t \quad (30)$$

are now introduced. In Laplace space, the equation of motion (eq 14) becomes

$$\delta\bar{\mathbf{u}}(\mathbf{r},s) = \left[\frac{\bar{\nu}(s)}{\rho s^2}\right]\nabla[\nabla\cdot\delta\bar{\mathbf{u}}(\mathbf{r},s)] - \left[\frac{\bar{\mu}(s)}{\rho s^2}\right]\nabla\times[\nabla\times\delta\bar{\mathbf{u}}(\mathbf{r},s)] \quad (31)$$

and the boundary conditions in eqs 16−18 and 28 become

$$\delta\bar{\epsilon}_{\theta r}(r_c,s) = \delta\bar{\epsilon}_{\varphi r}(r_c,s) = \delta\bar{\epsilon}_{\theta r}(\infty,s) = \delta\bar{\epsilon}_{\varphi r}(\infty,s) = 0 \quad (32)$$

$$2\bar{\mu}(s)\frac{\partial\delta\bar{u}_r(\infty,s)}{\partial r} + [\bar{\nu}(s) - 2\bar{\mu}(s)]\nabla\cdot\delta\bar{\mathbf{u}}(\infty,s) = 0 \quad (33)$$

$$2\bar{\mu}(s)\frac{\partial\delta\bar{u}_r(r_c,s)}{\partial r} + [\bar{\nu}(s) - 2\bar{\mu}(s)]\nabla\cdot\delta\bar{\mathbf{u}}(r_c,s) - 3K_c\frac{\delta u_r(r_{c,s})}{r_c} = -3K_c\frac{C(\theta,\phi)}{s} \quad (34)$$

D. Experimental Observables. Equations 31−34 define a model for the complete solvent response $\mathbf{u}(\mathbf{r}, t)$ to electronic excitation of the solute. However, we are interested in only one component of that response, the Stokes shift induced by the reaction of the solvent back on the solute. To calculate the Stokes shift, eq 26 is integrated to give a potential function for the movement of the cavity boundary in the ground state

$$U_g = {}^3/_2 K_s r_c \int \delta u_r^2(r_c,\theta,\varphi)\, d\Omega \quad (35)$$

where $d\Omega = \sin\theta\, d\theta d\varphi$. If U_0 is the vertical transition energy from the ground-state equilibrium position, the excited-state potential is

$$U_e = U_0 - 3K_s r_c^2 \int \delta u_r(r_c,\theta,\varphi)\, d\Omega + {}^3/_2 K_s r_c \int \delta u_r^2(r_c,\theta,\varphi)\, d\Omega \quad (36)$$

The electronic transition energy is given by the difference potential

$$\Delta U = U_e - U_g = U_0 - 3K_s r_c^2 \int \delta u_r(r_c,\theta,\varphi)\, C(\theta,\varphi)\, d\Omega \quad (37)$$

The time-dependent Stokes shift $S(t)$ is derived from the time-dependent solvent displacement field

$$S(t) = U_0 - \Delta U(t) = 3K_s r_c^3 \int [\delta u_r(r_c,\theta,\varphi;t)/r_c] C(\theta,\varphi)\, d\Omega \quad (38)$$

Frequently, we will be most concerned with the solvation response function, defined as

$$R(t) = \frac{S(t) - S(\infty)}{S(0) - S(\infty)} \quad (39)$$

Noticing that $\delta u_r(r_c,\theta,\varphi;\infty) = r_c C(\theta,\varphi)$ allows the response function to be written

$$R(t) = 1 - \frac{\int [\delta u_r(r_c,\theta,\varphi;t)/r_c] C(\theta,\varphi)\, d\Omega}{\int C^2(\theta,\varphi)\, d\Omega} \quad (40)$$

III. Solution of the Model

The model developed in the last section can be solved analytically without further approximation, as outlined in the Appendix. The complete solution decomposes into a summation of solutions for each multipole moment of the shape change. This expansion has an analog in the treatment of polar solvation,[46−48] where an arbitrary charge redistribution is expanded in multipole moments. In the nonpolar model, the $n = 0$ component represents a spherical change in size upon excitation. The even components with $n \geq 2$ represent various changes in shape with constant total volume. The components with n odd include a forced displacement of the solute center-of-mass. The time dependence of the Stokes shift depends only on n, the principle index of the spherical harmonic, which determines the shape change in the excited state. The Stokes shift is independent of the secondary index m, which determines the orientation of the shape change.

The solvation response function is the weighted average of response functions for each multipole component

$$R(t) = \sum_n w_n R_n(t) \quad (41)$$

$$w_n = \frac{\sum_m (c_n^m)^2}{\sum_{n,m} (c_n^m)^2} \quad (42)$$

where the c_n^m are the multipole moments of the coupling. The time dependence of each multipole response function is

$$R_n(t) = 1 - \int_0^t \chi_n(t')\, dt' \quad (43)$$

where $\chi_n(t)$ is given by eq A18.

Equation 43 shows that $\chi_n(t)$ is a generalized susceptibility or impulse response function for the solvation experiment. By the classical fluctuation−dissipation theorem,[49] it can be related to the equilibrium fluctuations of the Stokes shift

$$\chi_n(t) = -\frac{d}{dt}\frac{\langle \delta S_n(t)\, \delta S_n(0)\rangle}{\langle \delta S_n^2(0)\rangle} \quad (44)$$

Time domain experiments are typically reported in terms of the Fourier transform of the susceptibility

$$\hat{\chi}_n(\omega) = \int_0^\infty e^{-i\omega t}\chi_n(t)\, dt = \bar{\chi}_n(i\omega) \quad (45)$$

which is related to the Laplace transform by the second equality. The spectral density is defined as $-\mathrm{Im}\,\bar{\chi}(\omega)$.

Equations A18−A21 and 43 constitute a complete solution of the viscoelastic solvation model. The only input needed are the two time-independent moduli, $G(t)$ and $K(t)$. For simple exponential functions, the inverse Laplace transform from $\bar{\chi}_n(s)$ to $\chi_n(t)$ can be solved analytically (see section IV.C.), but for nonexponential functions a numerical inversion is necessary. The susceptibilities $\chi_n(t)$ are defined so as to decay to zero at infinite time, so a numerical inverse Laplace transform can be avoided by using eq 45 and an inverse Fourier transform.

This continuum model of nonpolar solvation can be contrasted with previous treatments of polar solvation. In the current model, a full equation of motion (eq 14) is used to calculate the complete solvent displacement field. The experimental susceptibility is then projected from the full solvent response. Previous continuum models of polar solvation have calculated the experimental susceptibility directly from the bulk dielectric susceptibility, avoiding a full equation of motion and the calculation of the complete solvent response.[11−17] This latter approach implicitly invokes a quasi-state approximation, in which the equivalent of the inertial term of eq 14 is set to zero.[44] However, dropping the inertial term precludes propagating, wavelike motion in the solvent and retains only the diffusive

relaxation contained in the time-dependence of the dielectric susceptibility itself. Because of this approximation, these earlier models did not predict inertial dynamics. Unfortunately, writing an appropriate equation of motion for polar solvation is more difficult than for nonpolar solvation and must be left to future work.

Although most of this paper is concerned with the normalized response function, eq A23 also contains an expression for the total magnitude of the equilibrium Stokes shift

$$S_n(\infty) = 3K_s r_c^3 \sum_m (c_n^m)^2 \tag{46}$$

Using parameters from the systems to which this model has been fit gives fractional changes in solute radii of 5−6% for both dimethyl-*s*-tetrazine in *n*-butylbenzene[26] and *s*-tetrazine in propylene carbonate.[32] Because this model assumes linear coupling, it does not distinguish whether this change represents an expansion or contraction. However, these systems also show a narrowing of the fluorescence relative to the absorption spectrum, which indicates a small nonlinear component to the coupling. By the arguments of Nowak and Bernstein, the sign of the nonlinearity indicates a contraction, rather than an expansion.[50] Li, Lee, and Bernstein used other methods to estimate a very similar value of 5−10% for the change in the effective radius of benzene in alkanes.[51] These sizes changes are small enough that the assumption of weak coupling should be accurate.

IV. Phonon vs Structural Dynamics

A. Time Scales. Before specializing to specific examples, we will show that the separation of solvation dynamics into phonon and structural components is a general prediction of this model. We wish to emphasize that two time scales for solvation occur even when there is only one dissipative time scale for the liquid itself. Thus, we assume that a single time scale can characterize the relaxation of the moduli (see eq 9)

$$\tau_s = \frac{\eta}{G_\infty} \tag{47}$$

even though more complicated relaxation is important in many systems. We will also focus on the $n = 0$ component, which involves only longitudinal solvent motion, so it is clear that the existence of phonon and structural time scales is not related to the existence of longitudinal and transverse components of a vector field. Analogous results for $n \geq 1$, which also involve transverse solutions, are cited later.

Begin with the exact $n = 0$ solution from eq A18,

$$\bar{\chi}_0(s) = \frac{3K_s(1 - iy)}{[3K_s + 4\bar{\mu}(s)](1 - iy) - x^2\bar{\mu}(s)} \tag{48}$$

The time scale τ_s associated with $G(t)$ and $K(t)$ can range from ∼300 fs for low-viscosity liquids to ∞ for a glass (eq 47). In addition, there are two other times associated with this solution

$$\tau_l = r_c[\rho/(K_\infty + {}^4/_3 G_\infty)]^{1/2} \tag{49}$$

$$\tau_t = r_c[\rho/G_\infty]^{1/2} \tag{50}$$

These represent the time for longitudinal and transverse sound waves, respectively, to travel a distance of one solute radius, if the moduli are at their short time values. Taking typical values for a nonassociated liquid[52,53] and a benzene-sized solute (see Figure 2) give $\tau_t = 275$ fs and $\tau_l = 160$ fs. These times are of the magnitude expected for phonon-induced solvation.

B. Phonon-Induced Solvation. The roles of these three times becomes clearer in the limit where there is a large separation between the phonon-propagation times and the relaxation time of the moduli, i.e., $\tau_l, \tau_t \ll \tau_s$. In the short time or large *s* limit ($s\tau_s \gg 1$), the moduli approach the values $\bar{\mu}(s) \rightarrow G_\infty$ and $\bar{\nu}(s) \rightarrow M_\infty$. In this limit

$$x = is\tau_l \tag{51}$$

$$y = is\tau_l \tag{52}$$

Equation 48 reduces to

$$\bar{\chi}_0(s) \rightarrow (1 - f)\bar{\chi}_0^{\,ph}(s) \tag{53}$$

where the normalized phonon susceptibility is

$$\bar{\chi}_0^{\,ph}(s) = \frac{1 + s\tau_l}{1 + s\tau_l + s^2\tau_l^2[(1 + \beta^2)/(4\beta^2)]} \tag{54}$$

$$\beta^2 = 3\frac{M_\infty + (K_s - K_\infty)}{M_\infty - 3(K_s - K_\infty)} \tag{55}$$

$$f = \frac{{}^4/_3 G_\infty}{K_s + {}^4/_3 G_\infty} \tag{56}$$

Equations 53 and 54 can be analytically transformed back into the time domain. In the case where the solute force constant is small, $K_s < K_\infty + (1/3)M_\infty$, the response function is

$$R_0(t) = (1 - f)R_0^{\,ph}(t) + f \tag{57}$$

$$R_0^{\,ph}(t) = \exp\left(\frac{-t}{\tau_{ph}}\right)\left[\cos\left(\frac{t}{\beta\tau_{ph}}\right) - \beta \sin\left(\frac{t}{\beta\tau_{ph}}\right)\right] \tag{58}$$

$$\tau_{ph} = \frac{1 + \beta^2}{2\beta^2}\tau_l \tag{59}$$

The total response function along with the corresponding susceptibility is illustrated in Figure 2 for typical values of the parameters. The response function shows a rapid decay followed by weak, underdamped oscillations, settling to a nonzero value at long time.

In the case where the solute force constant is large, $K_s > K_\infty + (1/3)M_\infty$, β is imaginary. Taking $\beta'' = \mathrm{Im}\ \beta$, the response function is

$$R_0^{\,ph}(t) = \left(\frac{\beta'' + 1}{2}\right)\exp\left[\frac{-2\beta''t}{(\beta'' - 1)\tau_l}\right] - \left(\frac{\beta'' - 1}{2}\right)\exp\left[\frac{-2\beta''t}{(\beta'' + 1)\tau_l}\right]; \quad \beta'' > 1 \tag{60}$$

The response still overshoots the long time asymptote but returns to the asymptote in an overdamped fashion, without oscillations.

Qualitatively, the solution is in accord with the rapid component seen in both experiment and simulation of nonpolar solvation. The decay is subpicosecond in agreement with experiment.[27−33] The time scale of the decay is similar to the initial decay times found in simulations of nonpolar solvation.[19,23,24] Weak oscillations are predicted under some, but not

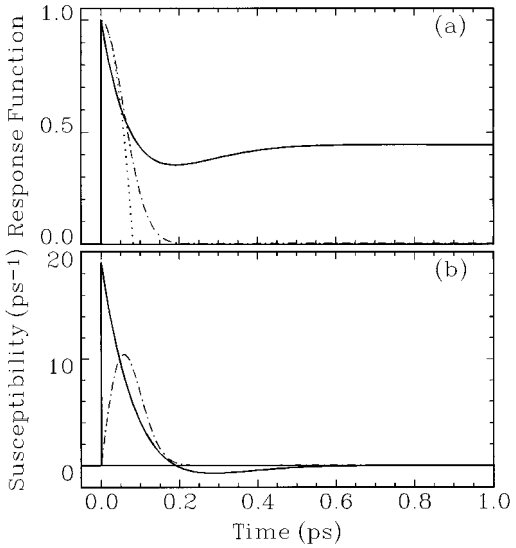

Figure 2. Short time, phonon approximation for nonpolar solvation dynamics on the inertial time scale (solid curves): (a) the total response function, (b) the phonon-induced susceptibility. Ballistic dynamics (dotted curve) have the correct $t \rightarrow 0$ behavior but diverge at long times. The Gaussian approximation (dot-dashed curves) converges at long times but does not capture the damped oscillations or nonzero asymptote predicted by the phonon approximation. The curves are calculated for a typical set of parameters, $r = 3$ Å, $\rho = 1$ g/cm^2, $G_\infty = 1.2 \times 10^{10}$ dyn/cm^2, $K_\infty = (5/3)G_\infty$, $K_s = K_\infty$. The ballistic time, $\tau_b = 58$ fs, was chosen for illustrative purposes.

all, conditions, in accord with simulation.[19,23,24] The decay is independent of the solvent viscosity and persists even in a glass, as is found experimentally.[27−33]

This model provides a simple physical picture for the origin of these features. In the current approximation, dynamics result from the propagation of waves in a purely elastic material. The sudden increase in solute forces at $t = 0$ launches an acoustic wavepacket, i.e., creates phonons. This process allows a partial expansion of the solute cavity and a partial decay of the solvation response function. The time scale of the decay is determined by the time needed for the phonon wavepacket to propagate away from the solute, i.e., τ_l. (The corresponding transverse time τ_t only occurs in $n \geq 1$ solutions. See section IV.D.) The oscillations in the response function result from the back-reaction of the tail of the oscillating wavepacket on the solute cavity. In real solvents, the wavepacket damps quickly after leaving the solute, but this is not important to the solvation process. The solvation decay does not represent a dissipative relaxation within the solvent, but rather a phonon-propagation time. The solvation does not result from dissipation of the solute energy directly into thermal energy but from a transfer of energy into a coherent solvent excitation.

Further expansion of the cavity requires dissipative, viscous flow and occurs on a longer time scale. The fraction of the expansion accomplished by phonon creation is given by f in eq 53. In the terminology of scattering experiments, f is the Debye−Waller factor, i.e., the fraction of the scattering in the quasielastic peak. It is determined by the strength of the solvent−solute force constant relative to the shear modulus of the solvent (eq 56). A stronger solute−solvent force constant is able to expand the solute cavity more effectively by elastic processes, and a greater fraction of the solvation is due to phonon creation.

Although the continuum model is good at reproducing most of the general properties of the short time solvation dynamics, it is qualitatively in error at the very earliest times. This is most easily seen in Figure 2b. The susceptibility should be continuous across $t = 0$, but the continuum prediction undergoes a step discontinuity. This error also shows up in the response function (Figure 2a) as a nonzero derivative at $t = 0$ and in the spectral density (Figure 3) as a too slow decay at high frequencies.

The correct limiting behavior of the response function is[54]

$$R(t) = 1 - \frac{t^2}{2\tau_b^2} + ... \tag{61}$$

The quadratic term represents the free streaming motion of the molecules, without any influence from intermolecular forces, which is sometimes referred to as ballistic dynamics.[18] A simple truncation of eq 61 diverges at long time. The simplest way to form a well-behaved response function is to complete eq 61 as a Gaussian[4]

$$R_G(t) = \exp\left(\frac{-t^2}{2\tau_b^2}\right) \tag{62}$$

These two approximations are illustrated in Figure 2a,b as a contrast to the continuum prediction. The error in the continuum model is important for the first ∼100 fs. After 100 fs, the continuum model is expected to give more reasonable results than the short time approximations. It contains the collective effects needed to describe oscillations and the halt at a nonzero value. A ballistic treatment does not represent these effects accurately.

The origin of the error in the continuum model is directly linked to the lack of molecular structure in the solvent. In a real solvent, the solute−solvent force acts directly on individual solvent molecules, each of which has a finite mass. The initial acceleration of these molecules is finite and determined only by the solute force and the mass of the molecules; changes in forces from other molecules are not felt at first. In the continuum model, there is no molecular structure, and therefore no minimum quantum of mass. The solute exerts a finite force on a sharp boundary, and the first infinitesimal layer of solvent experiences an infinite acceleration. This unphysical effect causes the incorrect behavior at early times.

From these observations, several comments can be made on classifying the time regions of solvation and the terminology used to describe them. On long time scales (>0.5 ps), relaxation is dominated by reorganization of the solvent structure and is accurately described as structural or dissipative relaxation. This process will be discussed in more detail in the next section. The fast solvation component (<500 fs) is due to the propagation of phonons and is accurately described as phonon-induced relaxation. The existence of this component is directly linked to the inclusion of inertial terms in the equation of motion of the solvent. Thus, it is also accurate to describe this relaxation as "inertial". The inertial relaxation is a collective property of the solvent and, at a qualitative level, does not require the inclusion of molecular structure in the solvent. The idea of "single-molecule" dynamics is incorrect for describing this entire time region. It fails to explain the halt of the relaxation at a nonzero value and does not permit oscillation in the response.

Single-molecule or "ballistic" dynamics are appropriate terms when eq 61 is a valid description. This time regime is confined to <100 fs and constitutes only a portion of the total inertial decay. It is only during this early time that the existence of molecular structure plays a primary role. At later times,

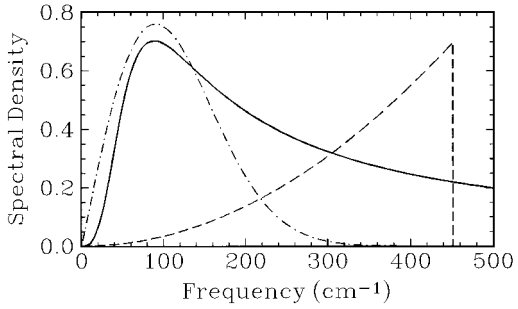

Figure 3. Spectral density predicted by the phonon approximation (solid curve). The spectral density does not have a simple relationship to the solvent density of states (dashed curve), which is simply the Debye density of states. The viscoelastic model does not have the correct high-frequency behavior, which is illustrated by the Gaussian approximation (dot-dashed curve). See Figure 2 for parameters.

molecular structure needs to be included for quantitative accuracy, but the major qualitative effects can be understood from a continuum point of view.

Originally, the terms ballistic[18] and inertial[4] dynamics were both coined to describe free-streaming motion. In subsequent usage, they have both been used to refer to all fast dynamics. In light of our arguments that free-streaming motion applies to only the earliest portion of the fast dynamics, we believe it is useful to reserve the term ballistic for free-streaming motion and to use inertial to describe all of the fast dynamics resulting from momentum effects in the solvent.

A final comment concerns the utility of the spectral-density representation as opposed to a time-domain representation. It has become increasingly common to convert time-domain data to the spectral-density representation. In part, the hope is that the spectral density from a specific experiment corresponds closely to the density of some type of intrinsic modes of the solvent, perhaps weighted by appropriate coupling factors.[55,56] Instantaneous normal modes are a popular candidate for the intrinsic modes.[57] Instantaneous normal modes are exact harmonic modes of the system at short times. In the continuum model, we have the advantage of knowing the instantaneous normal modes of the solvent exactly; they are the plane waves of Debye model.

The Debye density of states is plotted against the spectral density from the solvation experiment in Figure 3. Unfortunately, there is not a simple relationship between the two. In particular, the Debye frequency is not simply related to the phonon-induced solvation time. Although a coupling function could be defined so as to divide the spectral density into an intrinsic density and a coupling, the coupling function would be too complex for simple interpretation. In fact, the entire viscoelastic model presented here can be regarded as the calculation needed to obtain this coupling function, and the recognition of the existence of instantaneous normal modes does not reduce the complexity of the calculation.

C. Structural Relaxation. To complement the short time approximation that led to phonon relaxation in the last section, this section looks at a time course-grained approximation, again assuming a time-scale separation, $\tau_l, \tau_t \ll \tau_s$. The exact solution (eq 48) can be course-grained in time with respect to τ_t and τ_l by taking the limit $x,y \rightarrow 0$

$$\bar{\chi}_0(s) \rightarrow \frac{3K_s}{3K_s + 4\bar{\mu}(s)} = (1 - f) + f\bar{\chi}_0^{st}(s) \qquad (63)$$

In the time domain, the first, constant term in this expression translates into an instantaneous Stokes shift following excitation or a δ-function component in the response function

$$R_0(t) = (1 - f)\delta(t) + fR_0^{st}(t) \qquad (64)$$

It is a course-grained representation of the phonon-induced relaxation discussed in the previous section. The course-grained approximation contains information on the magnitude of the phonon-induced relaxation, but no details of its time dependence.

The structural susceptibility

$$\bar{\chi}_0^{st}(s) = \frac{1 - [\bar{\mu}(s)/G_\infty]}{1 + {}^4/_3[\bar{\mu}(s)/K_s]} \qquad (65)$$

and the corresponding structural response function $R_0^{st}(t)$ describes dissipative solvation at long times due to relaxation of the moduli, i.e., due to relaxation of the original solvent structure. It is unaffected by phonon propagation and is independent of the time scales τ_l and τ_s. The structural relaxation time scale is directly related to the shear relaxation time scale given by $G(t)$. In turn, the shear relaxation time scale is directly related to the solvent viscosity (eq 47). As the temperature is lowered, the structural solvation slows in proportion to the increasing viscosity and freezes in at the glass transition, where the viscosity diverges. This is in accord with the experimental observations of a long, viscosity-dependent component in nonpolar solvation.[27−34] It is interesting to note that the compression modulus does not appear in the expression for structural relaxation for $n = 0$; the relaxation is determined only by the shear relaxation function.

Further discussion of structural relaxation requires a specific model for $G(t)$. As a simple illustrative example, we introduce the Maxwell model,[45] which posits exponential relaxation of the shear modulus,

$$G(t) = G_\infty e^{-t/\tau_s} \qquad (66)$$

and

$$\bar{\mu}(s) = G_\infty \frac{s\tau_s}{1 + s\tau_s} \qquad (67)$$

For this model, eq 65 can be inverted analytically to give the course-grained solvation response function

$$R_0(t) = (1 - f)\delta(t) + f \exp\left[\frac{-t}{\tau_s/(1 - f)}\right] \qquad (68)$$

Figure 4 shows this function as well as the corresponding spectral density. The structural solvation time is proportional to, but not equal to, the shear relaxation time. In the case of an exponential shear relaxation function, the solvation response is also exponential. However, for nonexponential relaxation, the shapes of $G(t)$ and $R(t)$ differ.[26]

This model provides a simple physical interpretation of structural solvation. The initial expansion of the cavity by phonon creation creates strain within the effectively elastic solvent. Structural relaxation represents the release of that strain through viscous flow. Unlike the phonon-induced relaxation, structural relaxation is a directly dissipative transfer of energy into incoherent solvent energy. Although the dynamics of structural relaxation are approximately independent of the phonon-induced relaxation time, there is an essential interdependence between the processes. Phonon-induced solvation sets up the initial conditions for the structural relaxation, and as a

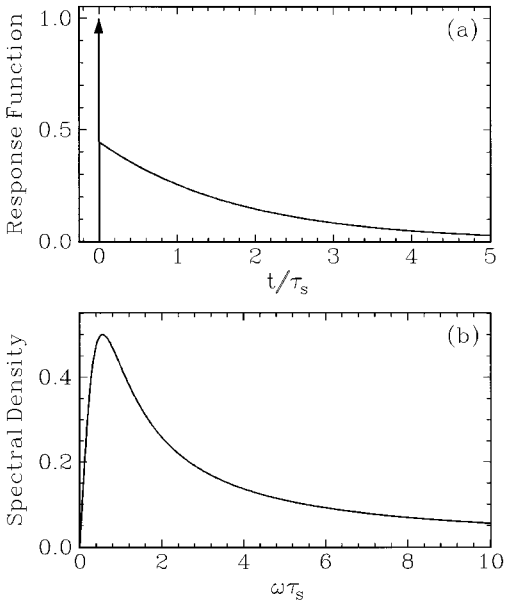

Figure 4. Time-course-grained, structural approximation to nonpolar solvation dynamics (solid curves): (a) the total response function, (b) the corresponding structural spectral density (Maxwell model, see Figure 2 for parameters).

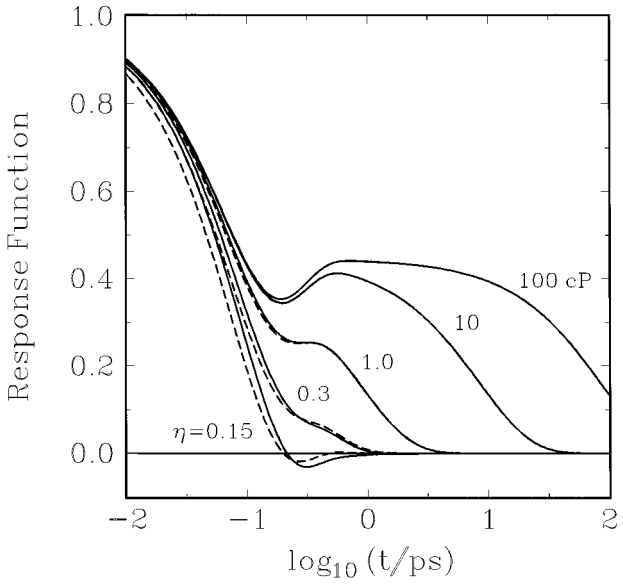

Figure 5. Exact solution of the continuum model for the solvation response function with Maxwell relaxation (solid) compared to the phonon−structure approximation (dashed) at several viscosities. The approximation becomes exact at high viscosity but develops modest errors at low viscosity. (See Figure 2 for parameters.)

result, the magnitude and rate of the structural solvation are dependent on the magnitude of the phonon-induced solvation.

D. Size vs Shape Changes. The discussion above was confined to size changes, $n = 0$. However, essentially the same analysis holds for shape changes, $n \geq 1$. In the $x,y \rightarrow 0$ limits, corresponding to structural relaxation, eqs 56, 64, and 65 still hold if the shear impulse response function $\bar{\mu}(s)$ is replaced by

$$\bar{\mu}_n(s) = \bar{\mu}(s)\,\frac{(n+2)}{4}\,\frac{(2n^2+1)\bar{\nu}(s) - 2n(n-1)\bar{\mu}(s)}{(n+1)(n+{}^1\!/_2)\bar{\nu}(s) + n\bar{\mu}(s)} \qquad (69)$$

and the high-frequency shear modulus G_∞ is replaced by $G_\infty{}^n = \bar{\mu}_n(\infty)$. The only important change is that both the longitudinal and shear impulse response functions are involved in the structural relaxation following a shape change, whereas only the shear modulus in involved with a size change. However, both moduli relax on a similar time scale and show a similar slowing at low temperatures and high viscosities, so the qualitative behavior of structural relaxation is the same, regardless of the value of n.

In the $s \rightarrow \infty$ case, corresponding to phonon-induced solvation, the formulas analogous to eq 54 become increasingly complex as n increases. However, only two time constants are involved. Both the longitudinal and shear wave propagation times, τ_l and τ_s, are involved for $n \geq 1$, whereas only τ_l is involved in the $n = 0$ case. However, τ_l and τ_s differ by only a factor of $(G_\infty/M_\infty)^{1/2}$. The two times are similar in magnitude, subpicosecond and independent of viscosity. Again the qualitative features of phonon-induced solvation are the same regardless of the value of n. The model predicts that the separation of the solvation dynamics into distinct phonon and structural components occurs for changes in shape as well as for changes in size.

V. Separability of Phonon and Structural Dynamics

A. Phonon−Structure Approximation. Examining the short and long time approximations in eqs 53 and 63 immediately suggests a simple approximation, in which the full response function is the sum of the phonon and structural limiting response functions

$$R_0(t) \approx (1-f)R_0{}^{\mathrm{ph}}(t/\tau_{\mathrm{ph}}) + fR_0{}^{\mathrm{st}}(t/\tau_s) \qquad (70)$$

This phonon−structure approximation has been used in previous comparisons of this theory to experimental data.[26,32] Within this approximation, the experimental response function can be decomposed into two processes with independent time scales and decay characteristics. The structural relaxation is unaffected by the phonon time τ_{ph}, and the phonon solvation is unaffected by the shear relaxation time τ_s. If the weak temperature dependence of G_∞ is neglected, the phonon solvation is independent of the solvent viscosity and temperature.

The accuracy of this approximation for the Maxwell model is examined in Figures 5 and 6 in the time and frequency domains, respectively. At large viscosities, the structural and phonon time scales are well separated, and the error in eq 70 is negligible. The structural and phonon components are clearly separated in both the time and frequency domains. At a moderate viscosity of 1 cP, the phonon and structural relaxation times are less well separated. A plateau no longer exists in the time domain, and the frequency domain peaks overlap. Nonetheless, the phonon−structure approximation remains accurate, and the response can be decomposed into two components. The approximation only breaks down at very low viscosities, where the structural and phonon times become very close.

B. An Exact Time-Scale Separation. Although the decomposition of the response into independent phonon and structural components breaks down at low viscosity, the ability to decompose the total response into two components is more robust. In Figure 6, a discernable shoulder exists even at 0.15 cP. Despite the small separation between phonon-induced and structural times and the significant error in the phonon−structure approximation, it still appears that the spectral density should be described as two overlapping peaks. In fact, it can be shown that decomposition into two peaks is still correct, even without a separation of time scales.

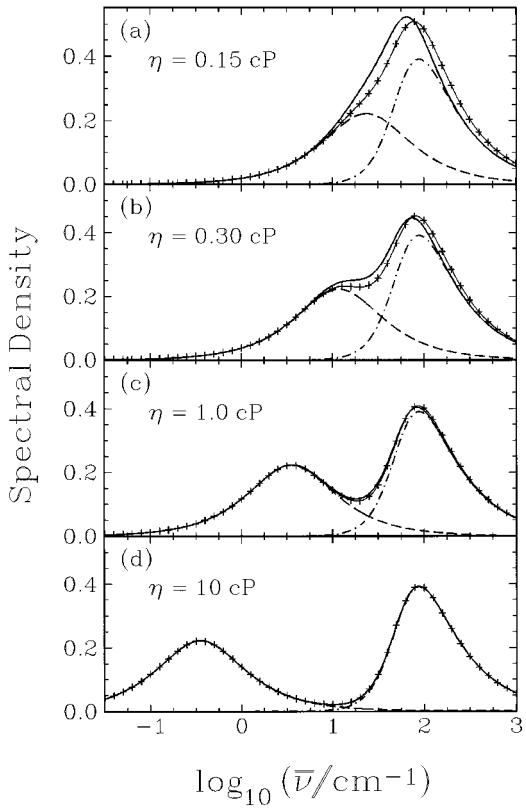

Figure 6. Exact solution of the continuum model for the solvation spectral density with Maxwell relaxation (solid) compared to the phonon−structure approximation (+) at several viscosities. The corresponding phonon (dash-dotted) and structural (dashed) components are also shown. The approximation becomes exact at high viscosity but develops modest errors at low viscosity. (See Figure 2 for parameters.)

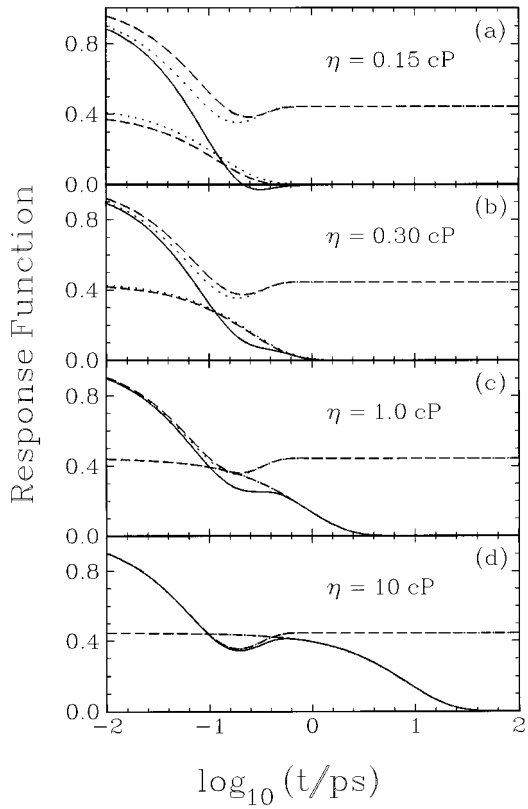

Figure 7. Two decompositions of the exact response function (solid) at several viscosities: the exact decomposition into fast and slow components (dashed) and the approximate decomposition into phonon and structural components (dotted). At high viscosity, the two decompositions become indistinguishable. For clarity, the amplitude of the structural and slow components *f* has been added to the phonon and fast curves.

Within the Maxwell model, the response can be exactly decomposed into fast and slow components, regardless of the relative sizes of the phonon and structural times

$$\bar{\chi}_0(s) = (1-f)\bar{\chi}_0^{\,\mathrm{fa}}(s\tau_{\mathrm{ph}};\, \tau_{\mathrm{ph}}/\tau_{\mathrm{s}}) + f\bar{\chi}_0^{\,\mathrm{sl}}(s\tau_{\mathrm{s}};\, \tau_{\mathrm{ph}}/\tau_{\mathrm{s}}) \quad (71)$$

$$\bar{\chi}_0^{\,\mathrm{fa}}(s\tau_{\mathrm{ph}};\, \tau_{\mathrm{ph}}/\tau_{\mathrm{s}}) = \chi_0^{\,\mathrm{ph}}(s\tau_{\mathrm{ph}}) + {}^1\!/_3 rfs\tau_{\mathrm{ph}}\left\{2\frac{\tau_{\mathrm{ph}}}{\tau_{\mathrm{s}}} + \frac{(s\tau_{\mathrm{ph}})^2}{f}\left[\frac{1 - {}^1\!/_3 rs\tau_{\mathrm{ph}}}{1 - s\tau_{\mathrm{ph}} - {}^1\!/_3 r(s\tau_{\mathrm{ph}})^2} - A^2(s\tau_{\mathrm{s}})\frac{B^{1/2}(s\tau_{\mathrm{s}}) - {}^1\!/_3 rA(s\tau_{\mathrm{s}})s\tau_{\mathrm{ph}}}{1 - B^{1/2}(s\tau_{\mathrm{s}})s\tau_{\mathrm{ph}} + {}^1\!/_3 rA(s\tau_{\mathrm{s}})(s\tau_{\mathrm{ph}})^2}\right]\right\} \quad (72)$$

$$\bar{\chi}_0^{\,\mathrm{sl}}(s\tau_{\mathrm{s}};\, \tau_{\mathrm{ph}}) = \bar{\chi}_0^{\,\mathrm{st}}(s\tau_{\mathrm{s}}) + r(1-f)\left(\frac{\tau_{\mathrm{ph}}}{\tau_{\mathrm{s}}}\right)^2 s\tau_{\mathrm{s}}\left[2 + \frac{1}{f}s\tau_{\mathrm{s}}(1 - A^2(s\tau_{\mathrm{s}}))\right] \quad (73)$$

$$A(s\tau_{\mathrm{s}}) = \frac{1 - s\tau_{\mathrm{s}}}{(1-f) - s\tau_{\mathrm{s}}} \quad (74)$$

$$B(s\tau_{\mathrm{s}}) = \frac{1 - s\tau_{\mathrm{s}}}{\frac{1-f}{r} - s\tau_{\mathrm{s}}} \quad (75)$$

$$r = \frac{K_\infty + {}^4\!/_3 G_\infty}{K_{\mathrm{s}} + {}^4\!/_3 G_\infty} \quad (76)$$

Examples of the decomposition of the total response into fast and slow components are shown in the time domain in Figure 7 and in the frequency domain in Figure 8. Each component still has its own time scale. The decay of R_0^{fa} is confined near τ_{ph} and the decay of R_0^{sl} is confined near τ_{s}, or in the frequency domain the fast component is peaked near $1/\tau_{\mathrm{ph}}$ and the slow component is peaked near $1/\tau_{\mathrm{s}}$.

For comparison to this exact decomposition, the approximate phonon−structure decomposition is also shown in Figures 7 and 8. Equations 72 and 73 show that the fast and slow components contain correction terms to the phonon and structure approximations. These terms vanish at high viscosity, where there is a large time-scale separation, $\tau_{\mathrm{ph}}/\tau_{\mathrm{s}} \ll 1$. This result emphasizes the fact that the phonon−structure approximation is the consequence of a time-scale separation, rather than of the smallness of a coupling term in the Hamiltonian.

Although a time-scale separation is required for the mathematical simplification of the phonon−structure approximation and for the interpretation of the two components as purely phonon and purely structural processes, a time-scale separation is not needed for the full response function to be exactly decomposable into a sum of components. The essential difference between the two decompositions is that in the approximate phonon−structure decomposition, the two components have independent shapes, whereas in the exact fast−slow decomposition, the time scale of one component affects the details of the shape of the other component. When external conditions such as the temperature or viscosity change, the phonon−structure approximation predicts that the components will simply shift in time. The exact result predicts that the two

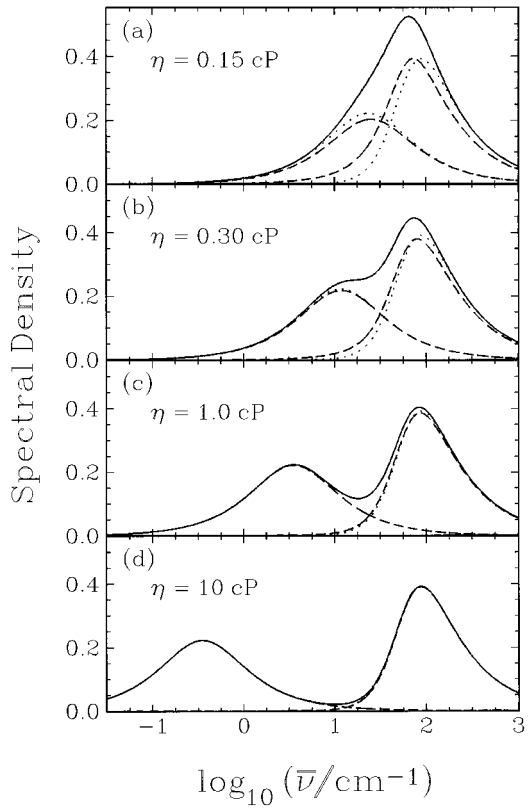

Figure 8. Two decompositions of the exact spectral density (solid) at several viscosities: the exact decomposition into fast, slow components (dashed), and the approximate decomposition into phonon and structural components (dotted). At high viscosity, the two decompositions become indistinguishable.

components will interact as their time scales become comparable, and simply scaling high-viscosity results in time will not be sufficient to predict the low-viscosity results.

VI. Spectroscopic vs Dynamical Approaches to Multiple Time Scales

The existence of phonon and structural time scales in nonpolar solvation dynamics is a specific example of the occurrence of multiple time scales in liquid dynamics, a theme that is currently prominent in a variety of contexts.[3−7] One method for analyzing these multiple time scales is what I will call the "spectroscopic" approach. This method has the greatest intuitive appeal when results are expressed as spectral densities and multiple time scales appear as multiple peaks in the frequency domain. In analogy with the analysis of optical spectra, each peak is assumed to be associated with a different coordinate. These coordinates are assumed to be independent in the sense that they allow a zeroth-order Hamiltonian for the system to be separated into a sum of independent terms. Higher order terms in the Hamiltonian cause damping of the coordinates and broadening of the peaks in the spectral density. In this approach, the essential approximation is that these higher order couplings are weak enough that the dynamics of each coordinate remains relatively simple.

The primary observable consequence of these assumptions is that the total spectral density or response function can be decomposed into the sum of two or more components. In addition, the components are completely independent. For example, their responses to changes in experimental conditions, such as temperature or viscosity, are not directly related. Multimode Brownian oscillator models are currently popular means of implementing this approach.[38]

If the spectroscopic approach is adopted, the essential problems are decomposing experimental results into the correct number of peaks and assigning each of the corresponding coordinates to specific molecular motions. Because the dynamics of each mode are assumed to be simple, the experimentally observable spectral density should be a direct representation of a complete set of coordinates or modes of the liquid filtered by a set of coupling constants, much as an infrared spectrum is a reflection of the complete set of molecular vibrations weighted by infrared cross sections. In the instantaneous normal mode approach, the description of liquids by such a set of modes has been proven to be accurate for sufficiently short time intervals.[54] However, arguments have also been made that such a set cannot be accurate for all times[58] and thus will not be able to deal with the problem of multiple time scales.

The viscoelastic continuum model of solvation presented here is a specific example demonstrating that the existence of multiple time scales does not require a spectroscopic explanation. It is an example of what I will call a "dynamical" approach. Because the continuum model is so simple, it is easy to see that there is not an undiscovered coordinate transformation that will bring it into correspondence with the spectroscopic approach.

In the continuum model of nonpolar solvation, the existence of two peaks in the spectral density is due to the inherently complex dynamics of a single coordinate, not due to two coordinates with simple dynamics. The cavity radius is the only collective solvent coordinate directly coupled to the solute. In the $n = 0$ case, only longitudinal motion is involved, so the longitudinal−transverse dichotomy is not responsible for the multiple time scales. For the Maxwell model, only a single relaxation time scale is assumed, so there is not a hidden assumption of multiple time scales in the input functions. Although the Hamiltonian for the solvent is approximately separable into an infinite set of zero-order modes for short time intervals, these modes do not have the direct relationship to the solvation spectral density that the spectroscopic approach seeks. In particular, the spectrum of short-time solvent eigenvalues by itself does not give any indication that two distinct time scales will be found in the model.

Within the current model of nonpolar solvation, the existence of multiple time scales is due to inherently complex dynamics along a single coordinate. The two components of the experimental response function are due to two different stages of relaxation: in this case, coherent phonon emission, followed by dissipative relaxation of the stresses created in the first stage.

The interpretation given above in terms of distinct phonon and structural relaxation processes is dependent on an assumption of a separation of time scales. However, the ability to decompose the spectral density into separate components is not dependent on this assumption. The exact solution of the continuum model decomposes into two components, even when the peaks in the spectral density are heavily overlapped. The components are directly interrelated in the sense that the magnitude and rate of the slower component depend on the conditions established by the faster component and in that changing the time scale of one component can alter the details of the peak shape of the other component. Thus the fact that a single experimental spectral density is well represented as a sum of components is not sufficient to prove that the underlying Hamiltonian separates into a sum of components or that the two components represent fully independent processes.

One approach to distinguishing between spectroscopic and dynamic explanations has been illustrated in Figure 5. At high viscosities and low temperatures, where a good time-scale

separation exists, suitable high-frequency (microscopic peak) and low-frequency (α peak) limiting forms can be fit to the well-separated peaks. In the spectroscopic approach, these forms can be simply scaled in frequency to generate results at low viscosity. In Figure 6, this procedure is represented by the phonon−structure approximation. In the dynamic approach, this procedure only generates an approximation to the true results, and deviations will be seen as the time-scale separation is decreased. This procedure has been applied frequently to neutron and light scattering and to dielectric relaxation, with the result that deviations often are seen at intermediate frequencies.[1] In spectroscopic terminology this represents a new component, β-relaxation, but from a dynamical point of view, it represents an essential interaction between the early and late stages of a complex relaxation.

Although this paper has focused on the simplest case of single-exponential structural relaxation, nonexponential relaxation is common, especially at high viscosity. The general comments made here can be applied to explaining multiple structural time scales. In a spectroscopic approach, the nonexponential decay is analyzed as a superposition of separate exponential decays. In a dynamical approach, it is regarded as an intrinsic property of a complex relaxation. Mode-coupling theory is such a dynamical theory for the form of structural relaxation.[59−61] Hole-burning experiments on nonpolar solvation have shown that mode-coupling theory is in agreement with the viscosity dependent changes in the form of the structural relaxation.[33,34] Recent work by Bhattacharyya and Bagchi has shown how multiple time scales arise in the mode-coupling treatment of the friction experienced by a diffusing particle.[62]

Another approach to distinguishing between spectroscopic and dynamical approaches is the use of high-order spectroscopies.[38] In the context of solvation, data on the hole-burning widths provides a higher order measurement related to the peak shifts calculated in this paper. Further experimental work is needed in this area. In nonresonant four- and six-wave mixing experiments, Steffen and Duppen have noted difficulties in reconciling the multiple time scales observed with Brownian oscillator models.[63] Further theoretical work is needed to determine if such results are indicative of a dynamical origin of the observed time scales.

VII. Summary

This paper has presented a continuum model for nonpolar solvation, which is an analog of continuum models of polar solvation.[8−17] It shows that the dynamics of nonpolar solvation depend on the relaxation of mechanical moduli in much the same way that the dynamics of polar solvation depend on dielectric relaxation. As is the case with polar solvation, the current model is expected to benefit from the addition of *k*-vector dependence to the moduli and nonspherical shapes to the solute cavity.[9] Generalized hydrodynamics[35] provides a route for systematically improving the viscoelastic model and making the connection to molecularly based theories.[18−25] Although lacking these refinements, the current model has the advantage of having compact, analytical solutions, which simplifies the discussion of the general trends and features of nonpolar solvation. In addition, the accuracy of the model is sufficient to interpret experiments[26,32] and computer simulations.[42]

Unlike previous continuum models of solvation, this model specifically addresses the issue of inertial dynamics. A full equation of motion, including both inertial terms and mechanical susceptibilities, was derived to describe the liquid dynamics. As a result, both a rapid viscosity-independent inertial process and a slower viscosity-dependent structural relaxation were predicted. In this model, the essential difference between these two processes is that the structural relaxation is strictly dissipative, whereas the inertial component is a coherent transfer of energy to well-defined solvent excitations (which decay dissipatively at a later time).

The success of a continuum model in describing short time dynamics should not be surprising. A good description of the velocity autocorrelation function can be obtained from a continuum model even in the 100 fs region.[36,37] As in the continuum model of solvation, errors in the limiting behavior are found at the very earliest times, but these comprise only a small fraction of the total correlation function. The fundamental physics at short times involves the propagation of sound waves, and the time scales are set by sound propagation times. To a first approximation, these times may be obtained in either a molecular description from molecular masses and intermolecular potentials or in a continuum description from the density and moduli.[64]

On the basis of the results of this model, several general comments were made about liquid dynamics. First, the idea of ballistic or single-molecule dynamics was distinguished from inertial dynamics. Many important features of inertial dynamics are captured in a continuum treatment, which lacks any molecular structure, but are not well represented by ballistic models. Conversely, a continuum picture does not treat the very early ballistic dynamics correctly. Inertial dynamics encompass a longer time regime than the short-time ballistic approximation does, and many of the important features of inertial dynamics are fundamentally collective.

Second, the results in this paper were presented in both the time domain and as spectral densities. Because the underlying modes of the continuum model are known exactly, it is easy to see that there is no simple relationship between the spectral density and intrinsic modes of the liquid. At least in the case of nonpolar solvation, the spectral-density representation does not appear to have any advantage over the time-domain representation.

Lastly, I contrasted spectroscopic and dynamical approaches to explaining the existence of multiple time scales in liquid dynamics. Despite major conceptual differences in these two approaches, the differences in predicted experimental results are subtle. In particular, both approaches predict that the observable response function or spectral density is decomposable into two components. Clearly, the ability to decompose experimental data into a sum of multiple components does not, by itself, demonstrate the existence of multiple solvation coordinates. Experiments specifically directed toward distinguishing these two approaches are needed.

Of course, this model by itself cannot prove the validity of these ideas in real liquids. However, this model does provide a specific example of an alternative to several currently popular methods of analyzing liquid dynamics. I hope it raises questions that will stimulate and direct further theoretical and experimental efforts to clarify the best approaches to understanding the dynamics of liquids and other complex systems.

Acknowledgment. This paper is based on work supported by the National Science Foundation under Grant No. CHE-9423935.

Appendix

Equation 31 is a standard vector wave equation, and with spherical boundary conditions, it can be solved analytically by

standard methods.[65] The first step is to expand the coupling in spherical harmonics

$$C(\theta,\varphi) = \sum_{m,n} c_n^{\,m} X_n^{\,m}(\theta,\varphi) \tag{A1}$$

We use complex spherical harmonics with δ-function normalization.[66] (Thus, for a purely spherical expansion, $c_n^{\,m} = \sqrt{4\pi}\delta r/r$.)

With the expansion of the coupling in multipole moments, the solvent displacement also decomposes into multipole moments

$$\delta\bar{\mathbf{u}}(\mathbf{r},s) = \sum_{m,n} c_n^{\,m} \delta\bar{\mathbf{u}}_n^{\,m}(\mathbf{r},s) \tag{A2}$$

where each component $\delta\bar{\mathbf{u}}_n^{\,m}(\mathbf{r},s)$ is a solution of eqs 31−34 with $X_n^{\,m}(\theta,\varphi)$ replacing $C(\theta,\varphi)$ in eq 34. Each component of the displacement is further expanded in vector spherical harmonics

$$\delta\bar{\mathbf{u}}_n^{\,m}(\mathbf{r},s)s/r_c = \bar{A}_L^{\,n}(s)\,\mathbf{L}_n^{\,m}(\mathbf{r}) + \bar{A}_M^{\,n}(s)\,\mathbf{M}_n^{\,m}(\mathbf{r}) + \bar{A}_N^{\,n}(s)\,\mathbf{N}_n^{\,m}(\mathbf{r}) \tag{A3}$$

Because only outgoing waves are anticipated, vector spherical harmonics of the third kind as defined by Morse and Feshbach are used.[65] They are defined in terms of the Hankel functions $h_n(r)$

$$\mathbf{L}_n^{\,m}(\mathbf{r}) = \nabla_{r_l}[h_n(\tilde{r}_l)\, X_n^{\,m}(\theta,\varphi)] \tag{A4}$$

$$\mathbf{N}_n^{\,m}(\mathbf{r}) = n(n+1)\frac{h_n(\tilde{r}_t)}{\tilde{r}_t} X_n^{\,m}(\theta,\varphi)\hat{\mathbf{r}} + [\tilde{r}_t \nabla_{r_t} X_n^{\,m}(\theta,\phi)]\frac{1}{\tilde{r}_t}\frac{\mathrm{d}}{\mathrm{d}\tilde{r}_t}[\tilde{r}_t h_n(\tilde{r}_t)] \tag{A5}$$

with the scaled distances

$$\tilde{r}_t = \left[\frac{-s^2\rho}{\bar{\mu}(s)}\right]^{1/2} r \tag{A6}$$

$$\tilde{r}_l = \left[\frac{-s^2\rho}{\bar{\nu}(s)}\right]^{1/2} r \tag{A7}$$

The $\mathbf{L}_n^{\,m}(\mathbf{r})$ are longitudinal solutions, and the $\mathbf{N}_n^{\,m}(\mathbf{r})$ are transverse solutions. The $\mathbf{M}_n^{\,m}(\mathbf{r})$ are torsional waves that are never excited by a quasi-spherical solute with slip boundary conditions, i.e., $\bar{A}_M^{\,n}(s) = 0$.

With this basis set, it is a tedious, but straightforward, calculation to find the amplitudes in eq A3 that satisfy the boundary conditions in eqs 32−34. The results are

$$\bar{A}_L^{\,n} = \frac{3z^2 H_n(x)}{B_n(x,y)\,H_n(x) - n(n+1)D_n(y)\,E_n(x)} \tag{A8}$$

$$\bar{A}_N^{\,n} = \begin{cases} 0; & n = 0 \\ \dfrac{D_n(y)}{H_n(x)}\bar{A}_L^{\,n}; & n \geq 1 \end{cases} \tag{A9}$$

in terms of the unitless variables

$$x = isr_c[\rho/\bar{\mu}(s)]^{1/2} \tag{A10}$$

$$y = isr_c[\rho/\bar{\nu}(s)]^{1/2} \tag{A11}$$

$$z = isr_c[\rho/K_s]^{1/2} \tag{A12}$$

and the auxiliary functions

$$B_n(x,y) = \left(\frac{4}{x^2} + \frac{3}{z^2}\right)h_n'(y) + \left[1 - \frac{2n(n+1)}{x^2}\right]\frac{h_n(y)}{y} \tag{A13}$$

$$D_n(y) = h_n'(y) - \frac{h_n(y)}{y} \tag{A14}$$

$$E_n(x) = \frac{2}{x^2}h_n'(x) - \left(\frac{2}{x^2} + \frac{3}{z^2}\right)\frac{h_n(x)}{x} \tag{A15}$$

$$H_n(x) = h_n'(x) + [(x^2/2) - (n^2 + n - 1)]\frac{h_n(x)}{x} \tag{A16}$$

As implied by the notation, the amplitudes of the vector harmonics are independent of m. In the case of a size change ($n = 0$), the solution is completely longitudinal. However, in the case of a shape change ($n \geq 1$), both longitudinal and transverse solvent motions are excited.

The equations above give a complete solution for the time-dependent solvent displacement field throughout space. Calculating the Stokes shift only requires the radial component at the cavity boundary, which is given by

$$[\delta\bar{\mathbf{u}}_n^{\,m}(r_c,\theta,\varphi;s)]_r = r_c c_n^{\,m}\bar{\chi}_n(s)\, X_n^{\,m}(\theta,\varphi)/s \tag{A17}$$

where the important time/frequency dependence has been isolated into the function

$$\bar{\chi}_n(s) = \frac{3K_s U_n(x,y)}{[3K_s - 2(n-1)(n+2)\bar{\mu}(s)]U_n(x,y) - \bar{\mu}(s)x^2 V_n(x,y)} \tag{A18}$$

$$U_n(x,y) = P_{n+1}(x)\,P_{n+1}(y) - nP_{n+1}(x)\,P_n(y) - [(n+1) + (x^2/2)]P_n(x)\,P_{n+1}(y) + n(x^2/2)P_n(x)\,P_n(y) \tag{A19}$$

$$V_n(x,y) = P_{n+1}(x)\,P_n(y) + n(n+1)P_n(x)\,P_{n+1}(y) - [(x^2/2) + (n+1)(n-1)^2]P_n(x)\,P_n(y) \tag{A20}$$

$$P_n(z) = \sum_{j=0}^{n} \frac{(2n-j)!}{2^{n-j}(n-j)!j!}\binom{z}{i}^j \tag{A21}$$

Inserting eqs A17 and A2 into eq 38 shows that the total Stokes shift is the sum of Stokes shifts attributable to each of the multipole moments of the coupling

$$S(t) = \sum_n S_n(t) \tag{A22}$$

Each multipole component of the Stokes shift is simply related to $\chi_n(t)$

$$S_n(t) = 3K_s r_c^{\,3}[\sum_m (c_n^{\,m})^2]\int_0^t \chi_n(t')\,\mathrm{d}t' \tag{A23}$$

References and Notes

(1) Richert, R., Blumen, A., Eds. *Disorder Effects on Relaxational Processes: Glasses, Polymers, Proteins*; Springer-Verlag: Berlin, 1994.
(2) Fleming, G. R. *Chemical Applications of Ultrafast Spectroscopy*; Oxford University Press: New York, 1986.
(3) McMorrow, D.; Lotshaw, W. T.; Kenney-Wallace, G. A. *IEEE J. Quantum Electron.* **1988**, *24*, 443.
(4) Carter, E. A.; Hynes, J. T. *J. Chem. Phys.* **1991**, *94*, 5961.
(5) Rosenthal, S. J.; Xie, X.; Du, M.; Fleming, G. R. *J. Chem. Phys.* **1991**, *95*, 4715.
(6) Jimenez, R.; Fleming, G. R.; Kumar, P. V.; Maroncelli, M. *Nature* **1994**, *369*, 471.
(7) Horng, M. L.; Gardecki, J.; Papazyan, A.; Maroncelli, M. *J. Phys. Chem.* **1995**, *99*, 17311.
(8) Barbara, P. F.; Jarzeba, W. *Adv. Photochem.* **1990**, *15*, 1.
(9) Maroncelli, M. *J. Mol. Liq.* **1993**, *57*, 1.
(10) Stratt, R. M.; Maroncelli, M. *J. Phys. Chem.* **1996**, *100*, 12981.
(11) Bakhshiev, N. G. *Opt. Spectrosc.* **1964**, *16*, 446.
(12) Bakhshiev, N. G.; Mazurenko, Yu. T.; Piterskaya, I. V. *Opt. Spectrosc.* **1966**, *21*, 307.
(13) Mazurenko, Yu. T.; Bakhshiev, N. G. *Opt. Spectrosc.* **1970**, *28*, 490.
(14) Mazurenko, Yu. T. *Opt. Spectrosc.* **1974**, *36*, 283.
(15) Calef, D. F.; Wolynes, P. G. *J. Chem. Phys.* **1983**, *78*, 4145.
(16) Bagchi, B.; Oxtoby, D. W.; Fleming, G. R. *Chem. Phys.* **1984**, *86*, 257.
(17) van der Zwan, G.; Hynes, J. T. *J. Phys. Chem.* **1985**, *89*, 4181.
(18) Walsh, A. M.; Loring, R. F. *Chem. Phys. Lett.* **1991**, *186*, 77.
(19) Ladanyi, B. M.; Stratt, R. M. *J. Phys. Chem.* **1996**, *100*, 1266.
(20) Larsen, R. E.; David, E. F.; Goodyear, G.; Stratt, R. M. *J. Chem. Phys.* **1997**, *107*, 524.
(21) Kalbfleisch, T. S.; Ziegler, L. D.; Keyes, T. *J. Chem. Phys.* **1996**, *105*, 7034.
(22) Evans, G. T. *J. Chem. Phys.* **1995**, *103*, 8980.
(23) Saven, J. G.; Skinner, J. L. *J. Chem. Phys.* **1993**, *99*, 4391.
(24) Stephens, M. D.; Saven, J. G.; Skinner, J. L. *J. Chem. Phys.* **1997**, *106*, 2129.
(25) Bagchi, B. *J. Chem. Phys.* **1994**, *100*, 6658.
(26) Berg, M. *Chem. Phys. Lett.* **1994**, *228*, 317.
(27) Yu, J.; Berg, M. *J. Chem. Phys.* **1992**, *96*, 8741.
(28) Yu, J.; Earvolino, P.; Berg, M. *J. Chem. Phys.* **1992**, *96*, 8750.
(29) Yu, J.; Berg, M. *J. Phys. Chem.* **1993**, *97*, 1758.
(30) Fourkas, J. T.; Berg, M. *J. Chem. Phys.* **1993**, *98*, 7773.
(31) Fourkas, J. T.; Benigno, A.; Berg, M. *J. Chem. Phys.* **1993**, *99*, 8552.
(32) Ma, J.; Vanden Bout, D.; Berg, M. *J. Chem. Phys.* **1995**, *103*, 9146.
(33) Ma, J.; Fourkas, J. T.; Vanden Bout, D. A.; Berg, M. In *Supercooled Liquids: Advances and Novel Applications*; Fourkas, J. T., Kivelson, D., Mohanty, U., Nelson, K., Eds.; ACS Symposium Series 676; American Chemical Society: Washington, DC, 1997; Chapter 15.
(34) Ma, J.; Vanden Bout, D.; Berg, M. *Phys. Rev. E* **1996**, *54*, 2786.
(35) Boon, J. P.; Yip, S. *Molecular Hydrodynamics*; McGraw-Hill: New York, 1980.
(36) Zwanzig, R.; Bixon, M. *Phys. Rev. A* **1970**, *2*, 2005.
(37) Metiu, H.; Oxtoby, D. W.; Freed, K. F. *Phys. Rev. A* **1977**, *15*, 361.
(38) Mukamel, S. *Principles of Nonlinear Optics*; Oxford University Press: New York, 1995.
(39) Schwartz, B. J.; Rossky, P. J. *J. Chem. Phys.* **1994**, *101*, 6902.
(40) Schwartz, B. J.; Rossky, P. J. *J. Mol. Liq.* **1995**, *65/66*, 23.
(41) Schwartz, B. J.; Rossky, P. J. *J. Chem. Phys.* **1996**, *105*, 6997.
(42) Berg, M., in preparation.
(43) Reynolds, L.; Gardecki, J. A.; Frankland, S. J. V.; Horng, M. L.; Maroncelli, M. *J. Phys. Chem.* **1996**, *100*, 10337.
(44) Golden, J. M.; Graham, G. A. C. *Boundary Value Problems in Linear Viscoelasticity*; Springer-Verlag: Berlin, 1988.
(45) Tschoegl, N. W. *The Phenomenological Theory of Linear Viscoelastic Behavior: An Introduction*; Springer-Verlag: Berlin, 1989.
(46) Kirkwood, J. G. *J. Chem. Phys.* **1934**, *2*, 351.
(47) Beveridge, D. L.; Schnuelle, G. W. *J. Phys. Chem.* **1975**, *79*, 2562.
(48) Castner, E. W.; Fleming, G. R.; Bagchi, B.; Maroncelli, M. *J. Chem. Phys.* **1988**, *89*, 3519.
(49) Chandler, D. *Introduction to Modern Statistical Mechanics*; Oxford University Press: Oxford, 1987.
(50) Nowak, R.; Bernstein, E. R. *J. Chem. Phys.* **1987**, *86*, 3197.
(51) Li, F.; Lee, J.; Bernstein, E. R. *J. Phys. Chem.* **1982**, *86*, 3606.
(52) Litovitz, T. A.; Davis, C. M. In *Physical Acoustics*; Mason, W. P., Ed.; Academic Press: New York, 1965; Vol. IIA.
(53) Harrison, G. *The Dynamic Properties of Supercooled Liquids*; Academic: New York, 1976; Section 5.1.
(54) Stratt, R. M.; Cho, M. *J. Chem. Phys.* **1994**, *100*, 6700.
(55) Cho, M.; Rosenthal, S. J.; Scherer, N. F.; Ziegler, L. D.; Fleming, G. R. *J. Chem. Phys.* **1992**, *96*, 5033.
(56) Yang, T.-S.; Vöhringer, P.; Arnett, D. C.; Scherer, N. F. *J. Chem. Phys.* **1995**, *103*, 8346.
(57) Stratt, R. M. *Acct. Chem. Res.* **1995**, *28*, 201.
(58) Zwanzig, R. *Phys. Rev.* **1967**, *156*, 190.
(59) Götze, W. In *Liquids, Freezing Glass Transition*; Hansen, J. P., Levesque, D., Zinn-Justin, J.; Eds.; Elsevier Science B.V.: Amsterdam, 1991.
(60) Götze, W.; Sjögren, L. *Rep. Prog. Phys.* **1992**, *55*, 241.
(61) Götze, W.; Sjögren, L. *Trans. Theory Stat. Phys.* **1995**, *24*, 801.
(62) Bhattacharyya, S.; Bagchi, B. *J. Chem. Phys.* **1997**, *106*, 7262.
(63) Steffen, T.; Duppen, K. *Phys. Rev. Lett.* **1996**, *76*, 1224.
(64) Zwanzig, R.; Mountain, R. D. *J. Chem. Phys.* **1965**, *43*, 4464.
(65) Morse, P. M.; Feshbach, H. *Methods of Theoretical Physics*; McGraw-Hill: New York, 1953.
(66) Arfken, G. *Mathematical Methods for Physicists*; Academic Press: New York, 1970.